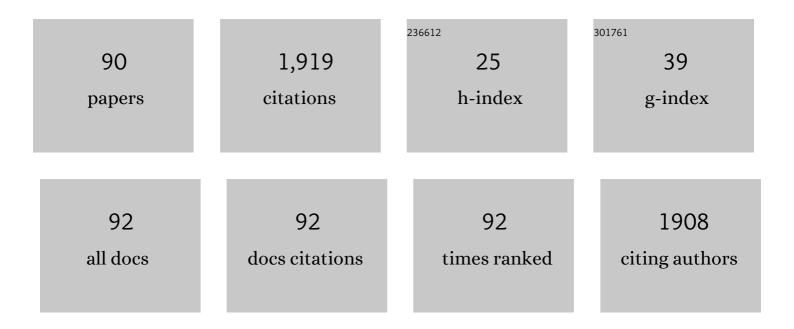
Christian Patzig

List of Publications by Year in descending order

Source: https://exaly.com/author-pdf/6380910/publications.pdf Version: 2024-02-01



#	Article	IF	CITATIONS
1	Sr[Li2Al2O2N2]:Eu2+—A high performance red phosphor to brighten the future. Nature Communications, 2019, 10, 1824.	5.8	248
2	Experimental evidence for an angular dependent transition of magnetization reversal modes in magnetic nanotubes. Journal of Applied Physics, 2011, 109, .	1.1	82
3	Surface-enhanced fluorescence from metal sculptured thin films with application to biosensing in water. Applied Physics Letters, 2009, 94, 063106.	1.5	65
4	Glancing angle sputter deposited nanostructures on rotating substrates: Experiments and simulations. Journal of Applied Physics, 2008, 104, .	1.1	61
5	Temporal Evolution of Crystallization in MgO–Al ₂ O ₃ –SiO ₂ –ZrO ₂ Glass Ceramics. Crystal Growth and Design, 2012, 12, 2059-2067.	1.4	59
6	The evidence of phase separation droplets in the crystallization process of a Li2O-Al2O3-SiO2 glass with TiO2 as nucleating agent – An X-ray diffraction and (S)TEM-study supported by EDX-analysis. Ceramics International, 2018, 44, 2919-2926.	2.3	52
7	Phase formation during crystallization of a Li2O-Al2O3-SiO2 glass with ZrO2 as nucleating agent – An X-ray diffraction and (S)TEM-study. Ceramics International, 2017, 43, 9769-9777.	2.3	51
8	Temporal Evolution of Diffusion Barriers Surrounding ZrTiO ₄ Nuclei in Lithia Aluminosilicate Glass-Ceramics. Crystal Growth and Design, 2012, 12, 1556-1563.	1.4	48
9	Mechanical, structural, and optical properties of PEALD metallic oxides for optical applications. Applied Optics, 2017, 56, C47.	2.1	42
10	Effect of the concentrations of nucleating agents ZrO2 and TiO2 on the crystallization of Li2O–Al2O3–SiO2 glass: an X-ray diffraction and TEM investigation. Journal of Materials Science, 2016, 51, 10127-10138.	1.7	40
11	Distribution of thulium in Tm3+-doped oxyfluoride glasses and glass-ceramics. CrystEngComm, 2013, 15, 6979.	1.3	39
12	Stages in the tribologically-induced oxidation of high-purity copper. Scripta Materialia, 2018, 153, 114-117.	2.6	39
13	Surface plasmon resonance from metallic columnar thin films. Photonics and Nanostructures - Fundamentals and Applications, 2009, 7, 176-185.	1.0	38
14	KLaF4 nanocrystallisation in oxyfluoride glass-ceramics. CrystEngComm, 2013, 15, 10323.	1.3	36
15	Crystallization of ZrO ₂ -nucleated MgO/Al ₂ O ₃ /SiO ₂ glasses – a TEM study. CrystEngComm, 2014, 16, 6578-6587.	1.3	35
16	Zr coordination change during crystallization of MgO–Al2O3–SiO2–ZrO2 glass ceramics. Journal of Non-Crystalline Solids, 2014, 384, 47-54.	1.5	34
17	The effect of TiO2 on nucleation and crystallization of a Li2O-Al2O3-SiO2 glass investigated by XANES and STEM. Scientific Reports, 2018, 8, 2929.	1.6	34
18	Temperature effect on the glancing angle deposition of Si sculptured thin films. Journal of Vacuum Science and Technology A: Vacuum, Surfaces and Films, 2008, 26, 881-886.	0.9	31

#	Article	IF	CITATIONS
19	Influence of substrate temperature on glancing angle deposited Ag nanorods. Journal of Vacuum Science and Technology A: Vacuum, Surfaces and Films, 2010, 28, 1002-1009.	0.9	30
20	The formation of nanocrystalline ZrO2 nuclei in a Li2O-Al2O3-SiO2 glass – a combined XANES and TEM study. Scientific Reports, 2017, 7, 10869.	1.6	30
21	Periodically arranged Si nanostructures by glancing angle deposition on patterned substrates. Physica Status Solidi (B): Basic Research, 2010, 247, 1322-1334.	0.7	29
22	Ordered silicon nanostructures by ion beam induced glancing angle deposition. Journal of Vacuum Science & Technology B, 2007, 25, 833.	1.3	27
23	Formation of bimetallic gold-silver nanoparticles in glass by UV laser irradiation. Journal of Alloys and Compounds, 2018, 767, 1253-1263.	2.8	27
24	A modified B2O3 containing Li2O-Al2O3-SiO2 glass with ZrO2 as nucleating agent - Crystallization and microstructure studied by XRD and (S)TEM-EDX. Ceramics International, 2018, 44, 19818-19824.	2.3	27
25	Effect of Y2O3 and CeO2 on the crystallisation behaviour and mechanical properties of glass–ceramics in the system MgO/Al2O3/SiO2/ZrO2. Journal of Materials Science, 2015, 50, 1986-1995.	1.7	26
26	Tubular magnetic nanostructures based on glancing angle deposited templates and atomic layer deposition. Physica Status Solidi (B): Basic Research, 2010, 247, 1365-1371.	0.7	25
27	Surface Crystallization of a MgO/Y2O3/SiO2/Al2O3/ZrO2 Glass: Growth of an Oriented Î ² -Y2Si2O7 Layer and Epitaxial ZrO2. Scientific Reports, 2017, 7, 44144.	1.6	25
28	Oriented crystallization of a β-Quartz Solid Solution from a MgO/Al ₂ O ₃ /SiO ₂ glass in contact with tetragonal ZrO ₂ ceramics. RSC Advances, 2015, 5, 15164-15171.	1.7	24
29	Charge transfer-induced magnetic exchange bias and electron localization in (111)- and (001)-oriented LaNiO3/LaMnO3 superlattices. Applied Physics Letters, 2017, 110, 102403.	1.5	24
30	Growth of Si nanorods in honeycomb and hexagonal-closed-packed arrays using glancing angle deposition. Journal of Applied Physics, 2008, 103, .	1.1	23
31	Arbitrarily shaped Si nanostructures by glancing angle ion beam sputter deposition. Physica Status Solidi (B): Basic Research, 2010, 247, 1310-1321.	0.7	23
32	Variation of Zr-L _{2,3} XANES in tetravalent zirconium oxides. Journal of Physics Condensed Matter, 2013, 25, 165505.	0.7	21
33	A normal-incidence PtSi photoemissive detector with black silicon light-trapping. Journal of Applied Physics, 2013, 114, .	1.1	20
34	In Situ X-ray Absorption Spectroscopic Study of Fe@Fe _{<i>x</i>} O _{<i>y</i>} /Pd and Fe@Fe _{<i>x</i>} O _{<i>y</i>} /Cu Nanoparticle Catalysts Prepared by Galvanic Exchange Reactions. Journal of Physical Chemistry C, 2015, 119, 21209-21218.	1.5	20
35	Correlation of Interface Impurities and Chemical Gradients with High Magnetoelectric Coupling Strength in Multiferroic BiFeO ₃ –BaTiO ₃ Superlattices. ACS Applied Materials & Interfaces, 2017, 9, 18956-18965.	4.0	19
36	Redox effects and formation of gold nanoparticles for the nucleation of low thermal expansion phases from BaO/SrO/ZnO/SiO ₂ glasses. RSC Advances, 2018, 8, 6267-6277.	1.7	19

#	Article	IF	CITATIONS
37	Evidence of epitaxial growth of high-quartz solid solution on ZrTiO4 nuclei in a Li2O-Al2O3-SiO2 glass. Journal of Alloys and Compounds, 2018, 748, 73-79.	2.8	19
38	High-strength glass-ceramics in the system MgO/Al2O3/SiO2/ZrO2/Y2O3 – microstructure and properties. CrystEngComm, 2013, 15, 6165.	1.3	18
39	Characterizing the residual glass in a MgO/Al2O3/SiO2/ZrO2/Y2O3 glass-ceramic. Scientific Reports, 2016, 6, 34965.	1.6	18
40	Effect of double layer thickness on magnetoelectric coupling in multiferroic BaTiO ₃ -Bi _{0.95} Gd _{0.05} FeO ₃ multilayers. Journal Physics D: Applied Physics, 2018, 51, 184002.	1.3	15
41	Laser welding of sapphire wafers using a thin-film fresnoite glass solder. Microsystem Technologies, 2015, 21, 1035-1045.	1.2	14
42	Formation and implantation of gold nanoparticles by ArF-excimer laser irradiation of gold-coated float glass. Journal of Alloys and Compounds, 2018, 736, 152-162.	2.8	14
43	Determination of the spontaneous polarization of wurtzite (Mg,Zn)O. Applied Physics Letters, 2014, 104, .	1.5	13
44	Highly textured fresnoite thin films synthesized <i>in situ</i> by pulsed laser deposition with CO ₂ laser direct heating. Journal Physics D: Applied Physics, 2014, 47, 034013.	1.3	13
45	Heterogeneous nucleation of Ba1-xSrxZn2Si2O7 from a BaO/SrO/ZnO/SiO2 glass using platinum as nucleation agent. Journal of the European Ceramic Society, 2017, 37, 4801-4808.	2.8	13
46	Impact of magnetization and hyperfine field distribution on high magnetoelectric coupling strength in BaTiO ₃ –BiFeO ₃ multilayers. Nanoscale, 2018, 10, 5574-5580.	2.8	13
47	The titanium coordination state and its temporal evolution in Li2O–Al2O3–SiO2 (LAS) glasses with ZrO2 and TiO2 as nucleation agents - A XANES investigation. Ceramics International, 2020, 46, 3498-3501.	2.3	13
48	Enhanced Magnetoelectric Coupling in BaTiO3-BiFeO3 Multilayers—An Interface Effect. Materials, 2020, 13, 197.	1.3	13
49	Bulk Crystallization in a SiO2/Al2O3/Y2O3/AlF3/B2O3/Na2O Glass: Fivefold Pseudo Symmetry due to Monoclinic Growth in a Glassy Matrix Containing Growth Barriers. Scientific Reports, 2016, 6, 19645.	1.6	12
50	Insight on agglomerates of gold nanoparticles in glass based on surface plasmon resonance spectrum: study by multi-spheres T-matrix method. Journal of Physics Condensed Matter, 2018, 30, 045901.	0.7	12
51	Structural evolution of CaF2 nanoparticles during the photoinduced crystallization of a Na2O–K2O–CaO–CaF2–Al2O3–ZnO–SiO2 glass. Journal of Materials Science, 2017, 52, 13390-134	40 ^{1.7}	12
52	Heteroepitaxial Ge-on-Si by DC magnetron sputtering. AIP Advances, 2013, 3, .	0.6	11
53	The crystallization of MgO–Al2O3–SiO2–ZrO2glass-ceramics with and without the addition of Y2O3– a combined STEM/XANES study. RSC Advances, 2016, 6, 62934-62943.	1.7	11
54	TiO2(B) nanocrystals in Ti-doped lithium aluminosilicate glasses. Journal of Non-Crystalline Solids: X, 2019, 2, 100025.	0.5	11

#	Article	IF	CITATIONS
55	Depth-profiling of nickel nanocrystal populations in a borosilicate glass – A combined TEM and XRM study. Ultramicroscopy, 2019, 205, 39-48.	0.8	11
56	Silicon Nanocolumns on Nanosphere Lithography Templated Substrates: Effects of Sphere Size and Substrate Temperature. Journal of Nanoscience and Nanotechnology, 2009, 9, 1985-1991.	0.9	10
57	The effect of CeO2 on the crystallization of MgO-Al2O3-SiO2-ZrO2 glass. Materials Chemistry and Physics, 2018, 212, 60-68.	2.0	10
58	WO ₃ as a nucleating agent for BaO/SrO/ZnO/SiO ₂ glasses – experiments and simulations. CrystEngComm, 2018, 20, 4565-4574.	1.3	10
59	Magnetoelectric Coupling in Epitaxial Multiferroic BiFeO ₃ –BaTiO ₃ Composite Thin Films. Physica Status Solidi (B): Basic Research, 2020, 257, 1900613.	0.7	10
60	Coupling of Metals and Biominerals: Characterizing the Interface between Ferromagnetic Shape-Memory Alloys and Hydroxyapatite. ACS Applied Materials & Interfaces, 2015, 7, 15331-15338.	4.0	9
61	Two-dimensional Frank–van-der-Merwe growth of functional oxide and nitride thin film superlattices by pulsed laser deposition. Journal of Materials Research, 2017, 32, 3936-3946.	1.2	9
62	Core–shell structures with metallic silver as nucleation agent of low expansion phases in BaO/SrO/ZnO/SiO ₂ glasses. CrystEngComm, 2019, 21, 4373-4386.	1.3	9
63	Optical bandgap control in Al2O3/TiO2 heterostructures by plasma enhanced atomic layer deposition: Toward quantizing structures and tailored binary oxides. Spectrochimica Acta - Part A: Molecular and Biomolecular Spectroscopy, 2021, 252, 119508.	2.0	9
64	Patterning concept for sculptured nanostructures with arbitrary periods. Applied Physics Letters, 2009, 95, 103107.	1.5	8
65	lsotropic, high coercive field in melt-spun tetragonal Heusler Mn ₃ Ge. APL Materials, 2016, 4, 086113.	2.2	8
66	Nucleation efficacy and flexural strength of novel leucite glass-ceramics. Dental Materials, 2020, 36, 592-602.	1.6	8
67	Ion beam induced anisotropic deformation of Si nanosprings. Journal Physics D: Applied Physics, 2009, 42, 145404.	1.3	7
68	Effect of Al2O3 on phase formation and thermal expansion of a BaO-SrO-ZnO-SiO2 glass ceramic. Ceramics International, 2018, 44, 2098-2108.	2.3	7
69	Low Temperature Fusion Wafer Bonding Quality Investigation for Failure Mode Analysis. ECS Transactions, 2013, 50, 227-239.	0.3	6
70	The acceleration of crystal growth of gold-doped glasses within the system BaO/SrO/ZnO/SiO2. Journal of the European Ceramic Society, 2019, 39, 554-562.	2.8	6
71	Plastic strain relaxation and alloy instability in epitaxial corundum-phase (Al,Ga) ₂ O ₃ thin films on <i>r</i> -plane Al ₂ O ₃ . Materials Advances, 2021, 2, 4316-4322.	2.6	6
72	Sample preparation for analytical scanning electron microscopy using initial notch sectioning. Micron, 2021, 150, 103090.	1.1	6

#	Article	IF	CITATIONS
73	Comparative study of enhanced fluorescence from nano sculptured thin films. , 2008, , .		5
74	Ion beam sputter deposition of epitaxial Ag films on native oxide covered Si(100) substrates. Applied Surface Science, 2012, 258, 9617-9622.	3.1	5
75	Thermal stability of B-based multilayer mirrors for next generation lithography. Thin Solid Films, 2017, 642, 252-257.	0.8	5
76	Oriented surface nucleation in diopside glass. Journal of Non-Crystalline Solids, 2021, 562, 120661.	1.5	5
77	Noble metals Pt, Au, and Ag as nucleating agents in BaO/SrO/ZnO/SiO2 glasses: formation of alloys and core–shell structures. Journal of Materials Science, 2022, 57, 6607-6618.	1.7	5
78	Ferromagnetic phase transition and single-gap type electrical conductivity of epitaxial LaMnO ₃ /LaAlO ₃ superlattices. Journal Physics D: Applied Physics, 2017, 50, 43LT02.	1.3	4
79	Microstructure investigation and fluorescence properties of europium-doped scheelite crystals in glass-ceramics made under different synthesis conditions. Journal of Luminescence, 2021, 238, 118244.	1.5	4
80	Microspot surface enhanced fluorescence from sculptured thin films for control of antibody immobilization. Proceedings of SPIE, 2011, , .	0.8	3
81	Crystallization and microstructure of a glass seal for rapid laser sealing in the system CaO/Al2O3/SiO2. Journal of Materials Science, 2018, 53, 16207-16219.	1.7	3
82	Dünne Schichten durch Deposition unter streifenden Einfall. Vakuum in Forschung Und Praxis, 2010, 22, 14-19.	0.0	2
83	Enhancement of stiffness of vertically standing Si nanosprings by energetic ions. Journal of Applied Physics, 2010, 107, 094315.	1.1	2
84	X-ray Absorption Spectroscopic Studies of the Penetrability of Hollow Iron Oxide Nanoparticles by Galvanic Exchange Reactions. Journal of Physical Chemistry C, 2017, 121, 19735-19742.	1.5	2
85	Compositional study on the size distribution of nickel nanocrystals in borosilicate glasses. Journal of Non-Crystalline Solids, 2020, 549, 120357.	1.5	2
86	Silver doped glasses from the system BaO/SrO/ZnO/SiO2 – The influence of Sb, Sn, and Ta on the formation of core-shell structures. Ceramics International, 2021, 47, 1126-1132.	2.3	2
87	Periodic nanoscale Si structures by ion beam induced glancing angle deposition. , 2008, , .		1
88	Experimental evidence of wide bandgap in triclinic (001)-oriented Sn5O2(PO4)2 thin films on Y2O3 buffered glass substrates. Journal of Materials Chemistry C, 2020, 8, 14203-14207.	2.7	1
89	Swift Heavy Ion Irradiation Induced Effects in Si/SiOx Multi-Layered Films and Nanostructures. Materials Research Society Symposia Proceedings, 2009, 1181, 48.	0.1	0
90	Mechanical Characteristics of Silicon Nanostructures Using Force Distance Spectroscopy. Journal of Nanoscience and Nanotechnology, 2010, 10, 2994-3000.	0.9	0